Lithium-Ion Storage in Molybdenum Phosphides with Different Crystal Structure

Xiaozhe Jin, Ruixue Tian, Aimin Wu, Yadan Xiao, Xufeng Dong, Fangyuan Hu, Hao Huang*

Key Laboratory of Energy Materials and Devices (Liaoning Province), School of Materials Science and Engineering, Dalian University of Technology, Dalian 116024, Liaoning Province, China.

** Corresponding author. Email: huanghao@dlut.edu.cn.*

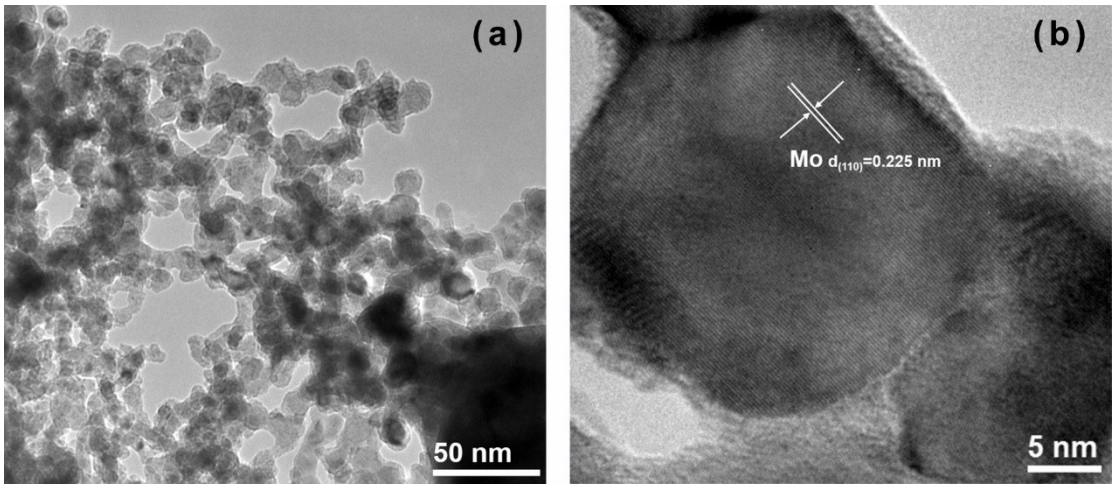

Figure S1. TEM images of Mo nanoparticles.

The microstructure of Mo nanoparticels as shown in the transmission electron microscope (TEM) image (Figure S1a) indicates the homogeneous spheres with the diameter of about 15-25 nm. The HRTEM image is shown in Figure S1b, in which the lattice fringes with the interval of around 0.225 nm are evidently observed, corresponding to the (110) lattice plane of cubic Mo crystalline.

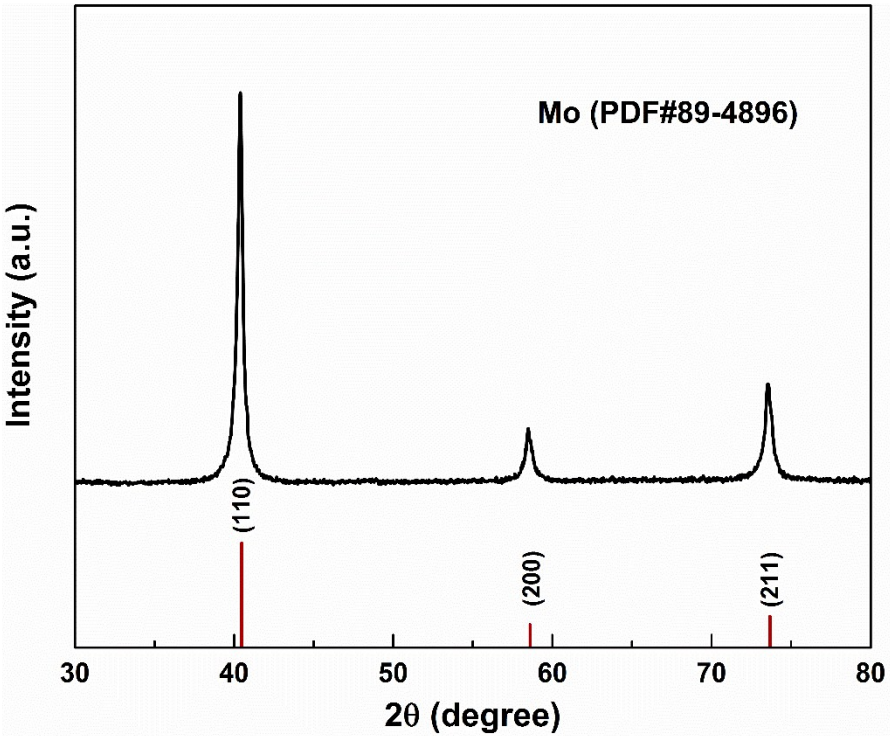

Figure S2. XRD pattern of Mo nanoparticles.

The XRD pattern of Mo nanoparticles is shown in Figure S2. The strong diffraction peaks at 40.36º, 58.48º and 73.56º can be indexed to cubic Mo (JPCDS 89-4896) with a space group of *Im-3m* with $a = b = c = 3.14$ Å.

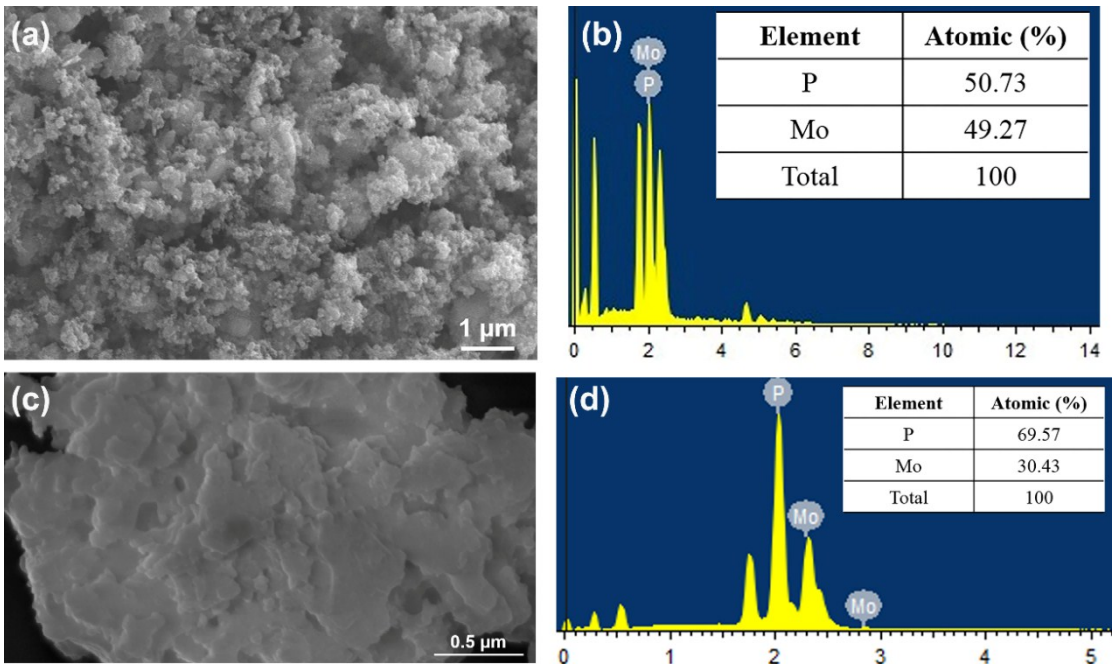

Figure S3. SEM images of (a) MoP nanoparticles and (c) MoP_2 nanosheets, the EDX spectra of (b) MoP and (d) MoP_2.

The SEM images of the MoP and MoP_2 as shown in Figure S3a and c suggest the morphology are nanosphere and nanosheet, respectively. The EDX spectra of MoP nanospheres and MoP_2 nanosheets (Figure S3b,d) confirm the Mo/P atomic ratios are about 1:1 and 1 : 2, respectively.

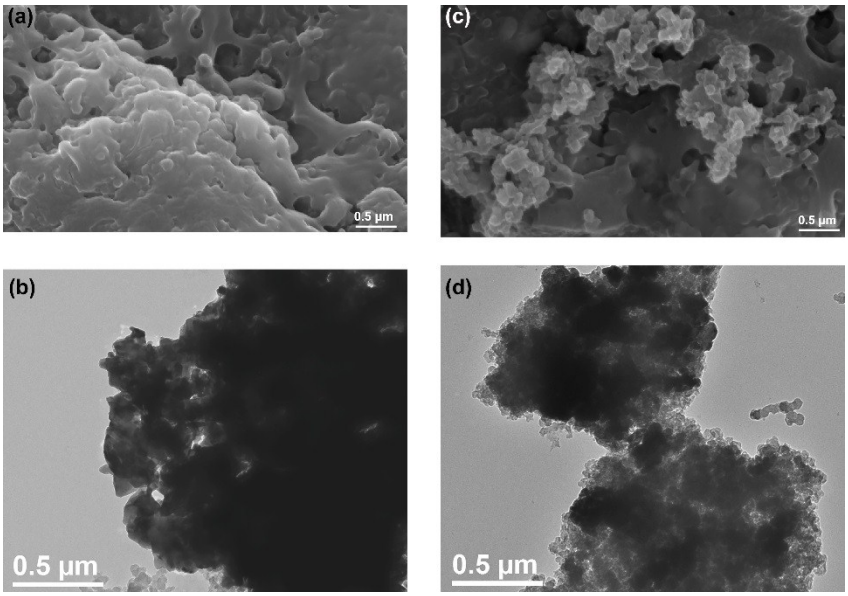

Figure S4. (a) SEM and (b) TEM images of MoP_2 electrode after 300 cycles at the current density of 0.1 A g^{-1}. (c) SEM and (d) TEM images of MoP electrode after 300 cycles at the current density of 0.1 A g^{-1}.

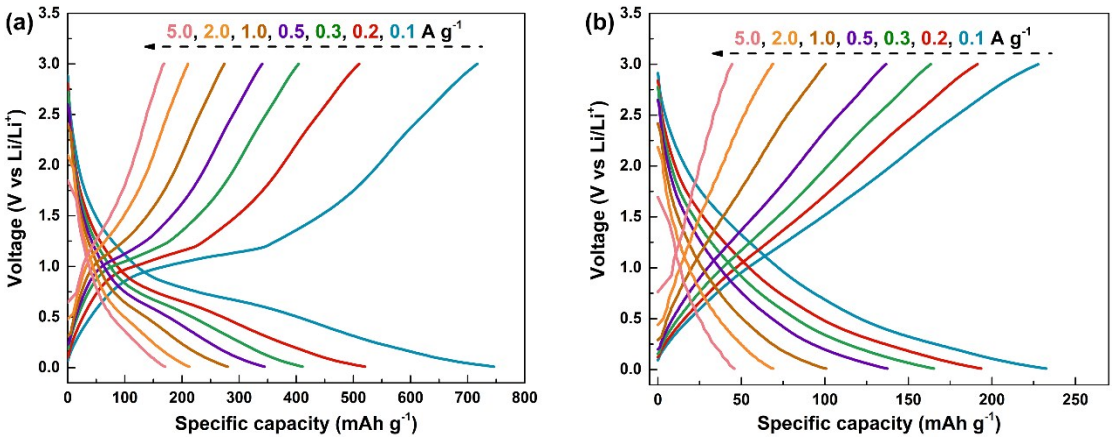

Figure S5. The discharge/charge curves at different current densities of (a) MoP_2 and (b) MoP electrodes.

As shown in Figure S4, MoP_2 electrode possess longer and flatter voltage plateaus at the current densities range of 0.1-5.0 A g^{-1} than MoP electrode.

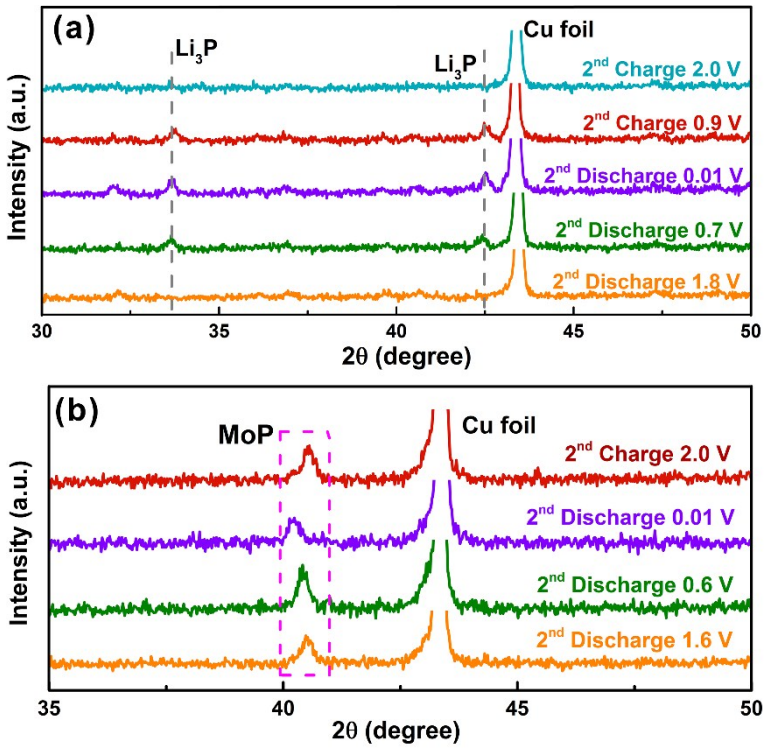

Figure S6. The *ex situ* XRD patterns of (a) MoP_2 and (b) MoP electrodes at different discharge/charge states during the second cycle.

As shown in Figure S5a, the *ex situ* XRD results suggest that Li_3P re-formed when MoP_2 electrode discharge to 0.7 and 0.01 V in the second cycle. Subsequently, the peaks of Li_3P fade away during delithiation step. The *ex situ* XRD of MoP at different discharge/charge state during the second cycle is shown in Figure S5b. The characteristic peaks corresponding to the MoP phase had a blue-shift with discharge to 0.01 V and returned to the initial location after delithiation.

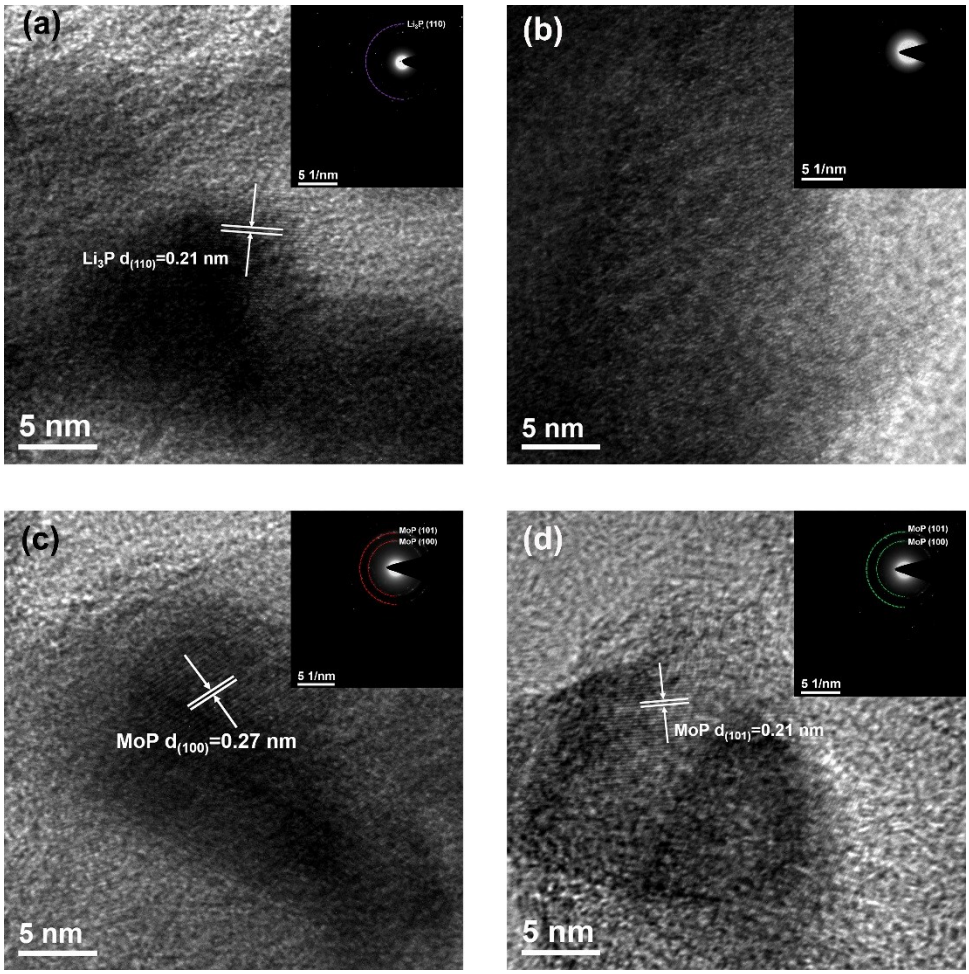

Figure S7. HRTEM images and corresponding SAED patterns of MoP_2 electrode when (a) discharge to 0.01 V and (b) charge to 2.0 V during the 1st cycle. HRTEM images and corresponding SAED patterns of MoP electrode when (c) discharge to 0.01 V and (d) charge to 2.0 V during the 1st cycle.

The HRTEM and SAED of the MoP_2 and MoP electrodes after cycles are shown in Figure S7. According to the HRTEM images of the MoP_2 electrodes after 1st discharge to 0.01 V (Figure S7a), a distinct lattice fringes with spacing of 0.21 nm, which is in accordance with the (110) plane of Li_3P. The selected area electron diffraction (SAED) pattern (inset of Figure S7a) can be matched (110) plane of Li_3P. However, no identifiable fringe can be observed in Figure S7b when the electrode charge to 2.0 V. The corresponding SAED pattern without diffraction ring (inset of Figure S7b) also reveals the poor crystallinity of the charging products. In addition, when the MoP electrode discharge to 0.01 V at the 1st cycle, obvious lattice fringes with distance of

0.27 nm corresponding to the (100) plane of MoP are observed (Figure S7c). Besides, SAED results as shown in the inset of Figure 6c exhibit the diffraction rings of (100) and (101) planes of MoP. The HRTEM images and SAED patterns of the MoP electrode charged to 2.0 V as shown in Figure S7d exhibit a lattice fringe with spacing of 0.21 nm which is in accordance with the (110) plane of MoP and a series diffraction rings corresponding to the (100) and (101) planes of MoP.

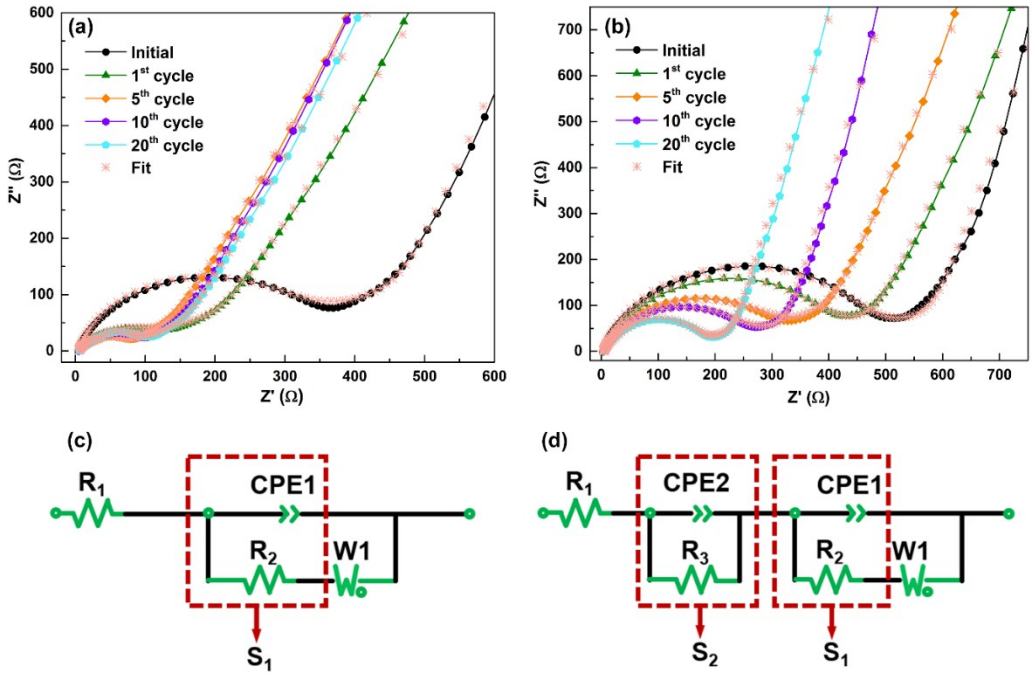

Figure S8. EIS spectra and their equivalent circuit fittings of (**a**) MoP_2 electrode and (**b**) MoP electrode, the equivalent circuit models of (**c**) initial electrode and (**d**) after cycle.

The charge transfer resistances (R_2) of MoP_2 and MoP electrodes according to the fitting data are recorded in Table S1. Faradic current density (I_F) of S_2 interface and the diffusion coefficient (D_0) of Li^+ are calculated in Equations (1-3) [1, 2] and recorded in Table S1.

$$Z' = R_1 + R_{ct} + \sigma\omega^{-0.5} \quad (1)$$

$$I_F = \frac{RT}{nAFR_{ct}} \quad (2)$$

$$D_0 = 0.5\left(\frac{RT}{AF^2\sigma C}\right)^2 \quad (3)$$

where R_{ct} is charge-transfer resistance, σ is the Warburg coefficient, ω is the angular frequency, T is the temperature (298 K), n is the number of electrons transferred per molecule during the redox reaction, A is the surface area of the electrode, F is the Faraday constant (96500 C mol^{-1}) and C is the molar concentration of Li ions. Both R_1

and R_{ct} are kinetics parameters independent of frequency. According to Equation (1), σ is the slope for the plot of Z' *vs.* the reciprocal square root of angular frequencies ($\omega^{-0.5}$).

Table S1. Equivalent circuit parameters of the MoP_2 and MoP electrodes in various cycles.

Sample	Cycle number	R_2 (Ω)	σ (Ω cm^2 s$^{-0.5}$)	D_0 ($cm^2\ s^{-1}$)	I_F ($mA\ cm^{-2}$)
Li/MoP_2 cell	Initial	310.60	88.53	1.91×10^{-12}	7.65×10^{-6}
	1st cycle	1.03	65.49	3.49×10^{-12}	2.29×10^{-5}
	5th cycle	0.85	58.00	4.45×10^{-12}	4.67×10^{-5}
	20th cycle	0.50	58.21	4.42×10^{-12}	3.80×10^{-5}
Li/MoP cell	Initial	467.40	148.79	6.78×10^{-13}	4.02×10^{-5}
	1st cycle	351.00	144.32	7.20×10^{-13}	4.34×10^{-5}
	5th cycle	299.50	140.94	7.55×10^{-13}	5.23×10^{-5}
	20th cycle	148.70	76.56	2.56×10^{-12}	9.25×10^{-5}

Table S2. Comparison of synthesis method and electrochemical performance of Mo-based anodes for Li-ion batteries.

Mo-based electrodes	Preparation routes	Voltage ranges	Electrochemical performances	Ref.
MoP_2 nanoparticle clusters	Ball milling	0~2.0 V	500 mAh g^{-1}, 0.2 C, after 60 cycles	3
MoP_2 nanoparticles	Ball milling	0~2.0 V	576.4 mAh g^{-1}, 0.1 C, after 100 cycles	4
MoP nanoparticles	Sol-gel method	0~3.0 V	252 mAh g^{-1}, 100 mA g^{-1}, after 100 cycles	5
MoO_3 nanoparticles	Hydrothermal method	0~3.0 V	~400 mAh g^{-1}, 500 mA g^{-1}, after 300 cycles	6
MoS_2 microspheres	Hydrothermal method	0~3.0 V	163 mAh g^{-1}, 100 mA g^{-1}, after 70 cycles	7
MoP_2 nanosheets	Plasma evaporation with phosphorization	0~3.0 V	676.60 mAh g^{-1}, 100 mA g^{-1}, after 300 cycles	**This work**
MoP nanospheres	Plasma evaporation with phosphorization	0~3.0 V	312.38 mAh g^{-1}, 100 mA g^{-1}, after 300 cycles	**This work**

REFERENCES

1. H. Huang, S. Gao, A.-M. Wu, K. Cheng, X.-N. Li, X.-X. Gao, J.-J. Zhao, X.-L. Dong and G.-Z. Cao, *Nano Energy*, 2017, **31**, 74-83.
2. X. Jin, H. Huang, A. Wu, S. Gao, M. Lei, J. Zhao, X. Gao and G. Cao, *ACS Nano*, 2018, **12**, 8037-8047.
3. M. G. Kim, S. Lee and J. Cho, *J. Electrochem. Soc.*, 2009, **156**, A89.
4. G. Park, S. Sim, J. Lee and S.-M. Lee, *J. Alloy. Compd.*, 2015, **639**, 296-300.
5. X. Wang, P. Sun, J. Qin, J. Wang, Y. Xiao and M. Cao, *Nanoscale*, 2016, **8**, 10330-10338.
6. F. Ma, A. Yuan, J. Xu and P. Hu, *ACS Appl. Mater. Interfaces*, 2015, **7**, 15531-15541.
7. S. Ding, D. Zhang, J. S. Chen and X. W. Lou, *Nanoscale*, 2012, **4**, 95-98.